Chemical Self-assembly for Electronic Applications

Janos H. Fendler

Department of Chemistry & CAMP, Clarkson University, Potsdam, New York 13699-5814

Received February 8, 2001. Revised Manuscript Received April 24, 2001

The current state of spontaneous formation of self-assembled monolayers (SAMs) on different substrates as well as on nanoparticles (referred to as monolayer-protected clusters, MPCs) is surveyed. Attention is then focused onto the assembly and self-assembly of nanoparticles (including MPCs), polymers, and polyelectrolytes into two-dimensional (2D) arrays and three-dimensional (3D) networks. Examples are given for the potential electronic applications of SAMs, MPCs, and the 2D and 3D structures fabricated from them and from polymers and polyelectrolytes. These examples include the formation of junctions, heterojunctions, and single-electron-transfer devices.

I. Introduction

Self-assembly implies the spontaneous organization of molecules, molecular clusters, and aggregate structures into two-dimensional (2D) arrays and three-dimensional (3D) networks by attractive forces or chemical bond formation. Biomineralization,[1,2] Mother Nature's self-assembly, provides a strikingly elegant and economic approach to the formation of 2D and 3D structures in desired sizes, shapes, and physical and chemical properties. The shiny and extremely tough structure of seashell, a protein−aragonite scafolding,[3] the highly desirable mechanical properties (strength-to-weight ratio, for example) of natural spider silk, a liquid-crystalline phase of fibroin assembled by noncovalent aggregation into a random coil,[4] and the precisely sized and linearly arranged iron oxide particles in magnetotactic bacteria[5] amply demonstrate the scope and versatility of biomineralization. No wonder chemists and material scientists have been inspired by biology and launched a mimetic approach to advanced materials preparation.[6,9]

Chemical self-assembly is driven by the potential benefits of fabricating electronic, optical, electro-optical devices, and sensors economically.[8] Requirements of the information industry (comprises computing, communication, measurement, and data storage) illustrates best the point. According to industry projections, computers by 2010 should be 256 times more capable as the current generation. Feature sizes of this computer will have to be well below the 100-nm range. It is increasingly recognized that current technologies will not be able to scale to this level and that chemical self-assembly will become the only economically feasible approach to the fabrication of components in the 30-nm range.

The purpose of the present review is to survey the current state of chemical self-assembly and illustrate some applications in electronics. Emphasis will be placed on self-assembled systems which have been shown to function both in solution and in the solid state. Thus, the self-association of surfactants into micelles, microemulsions, and vesicles (liposomes) will not be treated here. The interested reader is referred to published books and reviews.[6,8]

II. Chemically Self-assembled Systems

The benefits of chemical self-assembly are increasingly realized. This approach permits the fabrication of highly ordered, appropriately oriented 2D and 3D structures at a fraction of the cost of traditional band-gap engineering (molecular beam epitaxy, for example). Most importantly, it is versatile. A wide range of molecules and aggregated structures (nanoparticles or nanoplatelets, for example) having desired functional group moieties can be conveniently self-assembled. Furthermore, 3D structures can be constructed by combining several chemical methods (self-assembled alkanethiol monolayers and layer-by-layer self-assembled nanoparticles, for example) and even combining chemical and physical methods (depositing alkanethiol monolayers onto an ultrathin evaporated gold film, for example).

II.1. Self-assembled Monolayers (SAMs). Transferring a well-packed monolayer from aqueous solution surfaces to solid substrates was demonstrated a long time ago by the Langmuir−Blodgett (LB) technique.[10,11] LB-film formation is, however, cumbersome and time-consuming and requires a film balance. These problems have been overcome by the spontaneous formation of self-assembled monolayers (SAMs) on substrates.[12−15] Self-assembly is governed by the strong attraction (be it physisorption, chemisorption, or covalent bond formation) of an appropriately functionalized headgroup onto the substrate surface and by the hydrophobic interaction between the hydrocarbon tails of the molecules constituting the SAM. Formation of a SAM can be monitored, in situ, by electrochemical (quartz crystal microbalance, cyclic voltammetry, and impedance spectroscopy)[16,17] and optical (ellipsometry,[18] surface plasmon resonance imaging,[19] and infrared reflection absorption spectroscopy[20]) measurements. The structure of the SAM formed can be imaged, ex situ, by microscopic techniques (scanning electron and scanning force microscopies).[21]

Two different methods are practiced today for the spontaneous formation of SAMs on substrates. The first method involves the silanation of the substrate (typically glass) by surfactant silanes or siloxanes. Formation of sulfur coinage−metal (most often gold) covalent bonds

10.1021/cm010165m CCC: $20.00
Published on Web 07/18/2001

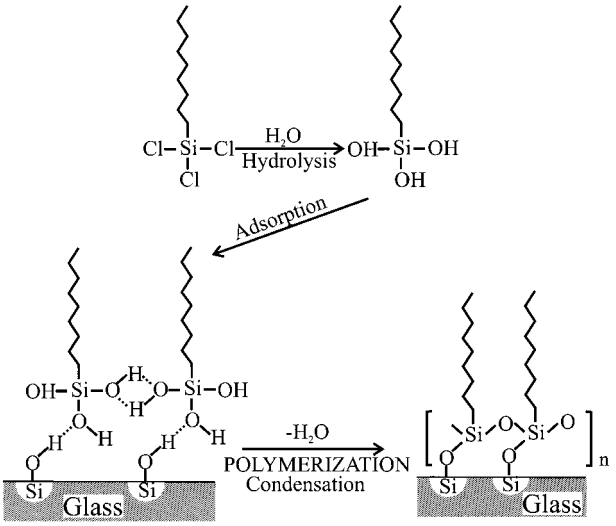

Figure 1. Schematics of OTS SAM formation on a glass substrate.

represents the second method of SAM formation. Both methods are attractive since they avoid the complex mechanical manipulation required for making LB films and since they are economical and amenable to scale-up. There is an additional important difference between LB films and SAMs. In LB film the configuration of the surfactants, determined by the parameters which are responsible for monolayer formation, is retained regardless of the type of substrate onto which the floating monolayer is transferred. In contrast, in SAMs the surfactant organization is primarily dependent on the nature of the substrate.

The spontaneous formation of a tightly packed monolayer upon the immersion of a substrate into a suitable solution was reported first by Sagiv and co-workers.[22] They immersed scrupulously clean glass, poly(vinyl alcohol), oxidized polyethylene, and evaporated aluminum substrates into millimolar solutions of *n*-octadecyltrichlorosilane (OTS) in an organic (80% *n*-hexadecane, 12% CCl_4, and 8% $CHCl_3$) solvent for a few minutes and obtained a well-packed SAM. The mechanism of self-assembly was discussed in terms of chemisorption and hydrolysis of the Si−Cl bonds at the substrate surface and subsequent formation of a network of Si−O−Si bonds (Figure 1). Recent theoretical and experimental studies established the energy offsets between a silicon conduction band and the lowest unoccupied molecular orbitals to be between 4.1 and 4.3 eV and that between the silicon valence band and the highest occupied molecular orbital of the alkyl chains to be between 4.1 an 4.5 eV in siloxane SAM, irrespective of the alkyl chain length (between C12 and C18).[23] These results validated the concept of using SAMs as ultrathin insulators and have been rationalized in terms of a good alignment between the carbon sp^3 and the silicon sp^3 orbitals and by assuming that the band structures of the carbon and silicon are almost centered on their respective sp^3 level.[23] Preferential adsorption of a silane surfactant from a mixture depends on the structures of the amphiphiles and the substrate. Self-assembly by physisorption is reversible, while that of chemisorption is irreversible. Thus, surfactants physisorbed in monolayers can be replaced by surfactants which are able to chemisorb. Such behavior was demonstrated by allowing a donor cyanine dye D (capable of physisorption) and OTS (known to chemisorb) to compete for binding sites on a given substrate. The ratio of OTS to D present in the SAM was found to increase with increasing time of substrate immersion into an organic solution containing fixed concentrations of D and OTS. This behavior indicated kinetically controlled physisorption of D and thermodynamically controlled chemisorption of OTS.[24] Removal of the reversibly adsorbed (physisorbed) D led to a skeletonized SAM with pinholes in the shape of D. Such pinholes can, in turn, serve as templates for other molecules (or nanoparticles) to self-assemble.[25] This approach opens the door, therefore, to chemical nanopatterning.[26]

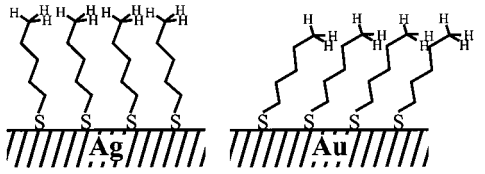

Figure 2. Schematics of alkanethiol SAMs on silver and gold substrates (showing tilt angles of 12° and 27°, respectively).

Immersion of a well-cleaned gold (or silver or copper, typically 200−400-nm thick, evaporated onto a 2−3-nm chromium-covered glass slide) substrate into an alcoholic solution of an organic thiol or dithiol results in the formation of a SAM. The immersion time, depending on the nature and concentration of the thiol (or dithiol) used, varies between minutes and days. Nonadsorbed thiol (or dithiol) molecules are removed by copious rinsing by alcohol to provide a stable long-lasting and defect-free SAM.

Examination of the adsorption of a mixture of thiol surfactants onto a gold substrate has provided useful insight into structure and mechanism of SAM formation. For example, SAMs assembled from a mixture of $-SH(CH)_{11}OH$ and $-SH(CH)_{19}OH$ had different composition-dependent wettabilities, indicating the absence of significant segregation on the gold surface.[27] Once again, lack of domain formation is typical for SAM films but it is a rarity for LB films. Electron diffraction and FTIR studies and computer simulations have established that the alkyl chains of alkanethiol-type (and dithiol-type) surfactants are tilted approximately 30° with respect to the gold substrate (and the sulfur atoms reside in the 3-fold hollows).[12] In contrast, SAMs formed from alkanethiol-type (and dithiol-type) surfactants on silver (or copper) substrates are not appreciably tilted (Figure 2).[28] However, rigid thiol SAMs behave differently; they have a relatively small tilt from either the gold or silver substrate normal. Quantitative FTIR of 4′-substituted-4-mercaptobiphenyls established the tilting of the biphenyl planes from the surface to be 14°, 20°, and 12° and rotation around the 1,4 axis of the ring to be 30°, 15°, and 30° for the NO_2, $C(O)CH_3$, and CO_2Et substituents on gold substrates.[29] On silver substrates, tilt angles for the NO_2, $C(O)CH_3$, and CO_2Et 4′-substituted 4-mercaptobiphenyl SAMs were found to be 8°, 21°, and 11°, respectively, while the rotation angles around the 1,4 axis of the ring were at 30°, 15°, and 30°.[29]

In closing this section, it is appropriate to mention that the formation of SAMs, particularly from thiols and dithiols on gold, is an established and mature technique.

Several hundred research papers and reviews have appeared and the structure of SAMs is well understood.[12,14,30−32] The extent of substrate coverage by SAMs (i.e., the extent of pinholes) can be conveniently determined by measuring the faradaic response of the $[Fe(CN)_6]^{3-}/[Fe(CN)_6]^{4-}$ redox couple in aqueous solution by cyclic voltammetry (employing the SAM-coated substrate as the working electrode). The cathodic (reduction) and anodic (oxidation) faradaic current peaks at the metal are completely suppressed in the presence of a defect-free SAM layer.[33,34]

II.2. Monolayer-Protected Clusters (MPCs). Stabilization of dispersed colloidal particles by surface treatments have been known for more than a century. Indeed, the beautiful deeply red colloidal gold dispersions, prepared by Michael Faraday sometime in the 1850s are still proudly displayed at the Royal Institution in London. Colloidal particles can be stabilized electrostatically and sterically.[35] The synergestic and concurrent particle preparation and electrostatic stabilization is illustrated by classical synthesis of 12-nm diameter gold particles.[36] The method involves the reduction of an aqueous gold chloride solution by sodium citrate. The gold particles formed are stabilized by an electrical double layer (composed of bulky citrate ions, chloride ions, and the cations attracted to them) responsible for the Coulombic repulsions which decays exponentially with increasing interparticle separations. There is a weak minimum in the van der Waals energy at an interparticle separation which approximately corresponds to the diameter of the stabilized gold nanoparticle. This minimum (where the attractive van der Waals forces are overcompensated by the repulsive electrostatic interactions) is responsible for the electrostatic stabilization of the gold colloids in dispersions. Steric stabilization is accomplished by adsorbing polymers and/or surfactants onto the surfaces of colloidal particles. Intertwining of the adsorbed polymers (and/or surfactant) in the interparticle space restricts the conformational motion (entropy effect) and increases local polymer concentration (which has to be compensated by solvation = osmotic effect) which, in turn, results in the stabilization of the particle. It should be pointed out that stabilization of colloidal particles by long-chain surfactants and/or polyelectrolytes involves *both* electrostatic and steric effects.[35,37] Preparation and characterization of nanoparticles and their assembly have been recently reviewed.[38]

Coating (capping or derivatization) by molecules which form chemical bonds with or chemisorb onto the particles provides an extremely useful method of nanoparticle stabilization.[30] Credit should be given to Brust and co-workers who prepared monolayer-coated gold nanoparticles (≤5 nm in diameter) by the sodium borohydride reduction of $AuCl_4^-$ in toluene−water in the presence of alkanethiols.[39] Significantly, this pioneering work has opened the door to treating nanoparticles as if they were simple molecules. Alkanethiols, mercapto alcohols, mercaptocarboxylic acids, and thiophenol(s) have been shown to be highly suitable capping agents for CdSe,[40,41] CdS,[42,43] ZnS,[44,45] maghematite,[46] Pd,[47] Ag,[48,49] and Au[50,51] nanoparticles (Figure 3). The capped nanoparticles can be separated from the dispersing solvent, stored as dried powders, and redispersed

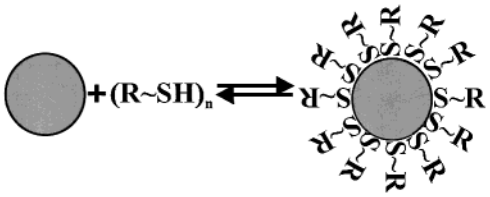

Figure 3. Schematics for the capping of a nanoparticle by alkanethiol molecules (i.e., the formation of MPCs).

on demand in a suitable solvent (polar solvent if the capping agent provides a hydrophilic surface and apolar solvent if the capping agent provides a hydrophobic surface) to form the same sized nanoparticles with the same degree of monodispersity.[52,53] Nucleophilic reagents have also been fruitfully employed as caps for nanoparticles.[54]

Murray and co-workers have coined the phrase of monolayer-protected clusters, MPCs, to describe the 3D analogs (i.e., monolayers on spherical nanoparticle substrate surfaces, see Figure 3) of 2D SAMs (i.e., monolayers on flat substrate surfaces).[53,55−62] Importantly, capping agents on nanoparticle surfaces can be exchanged by stronger ligands,[55,56,63]

$$(RS)_nMPS + x(R'SH) \rightarrow x(RSH) + (R'S)_x(RS)_{n-1}MPC \quad (1)$$

where x and n are the number of entering (stronger) and original (weaker) ligands, respectively. Citrate ions are readily replaced by a thiol ligand on gold nanoparticle surfaces, for example. This ligand-exchange reaction provides an important means for the chemical functionalization of the nanoparticles and greatly extends the versatility of these systems.[53,64] MPCs can be conveniently transferred from solvent to solvent, stored in the dried state, or organized (and self-organized) into 2D arrays or 3D networks on solid substrates. This versatility provides the potential for exploitation for catalytic, electronic, and optical applications. Thiol-functionalized oligonucleotides have also been shown to provide good monolayer coverage to gold nanoparticles (i.e., formed a good MPC!).[65] Formation of nanostructured metallic films have also been demonstrated by the self-assembly of carboxylate-functionalized alkanethiolate gold MPCs, using copper ion bridges, and the subsequent burning off of the organic materials (at <350° C).[66] It should be remembered, however, that surface properties of MPCs are different from those of their uncapped analogs (assuming that they can be prepared and examined!).

II.3. Self-assembly into 3D Networks. Adsorption (either by physisorption or by chemisorption) of nanoparticles onto a substrate is the simplest method of fabricating self-organized 2D arrays and/or 3D networks. Adsorption is accomplished by dropping a few drops of dilute nanoparticle dispersion onto a suitable substrate (casting) and evaporating the solvent (usually slowly and in a controlled environment).[67−69] Alternatively, the substrate is immersed into a dilute nanoparticle dispersion (for a time optimized for the adsorption), withdrawn, rinsed, and dried. Depending on the surface modifiers and on the dielectric constant of the medium, TiO_2 particles self-assembled into cubic arrays[70] or rodlike structures.[71] Silver nanoparticles have been

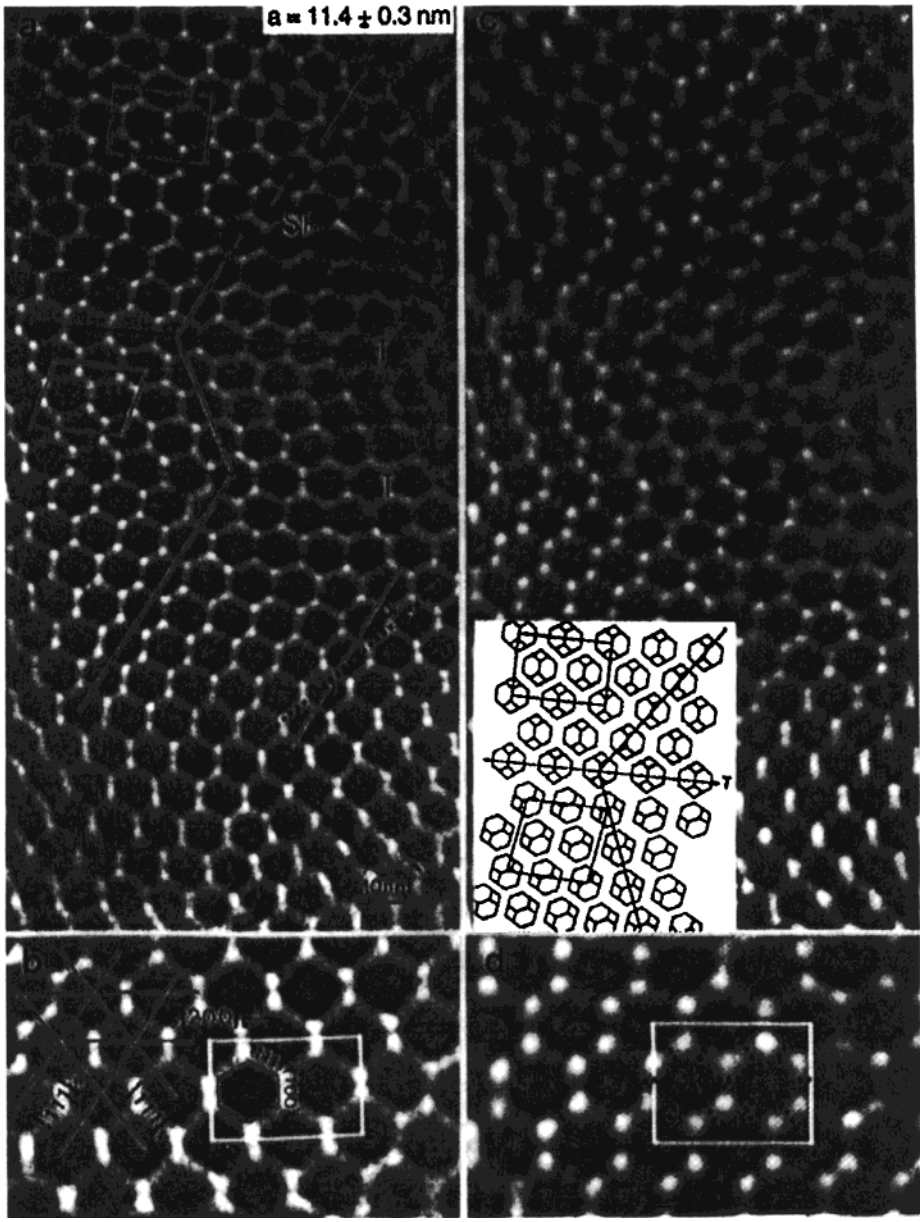

Figure 4. $[100]_s$ TEM images recorded from a single region of a silver nanocrystaline array (stabilized by dodecanethiol SAMs) under (a**)** in-focus and (c) out-of-focus conditions, showing the faceted shape and directional intermolecular bonds of the particles. The dark lines indicate (T) planes and the white−dark lines indicate the rotation of the $\{111\}_s$ plane across the twin plane and the region with stacking faults. A structural model for the formation of $\{100\}_s$ twins in the fcc superlattice is inset in (c). (b) and (d**)** are enlarged TEM images selected from (a) and (c), respectively, showing the relationship of the {111} and {100} facets of the truncated octahedron particles to the projected unit cell (white lines) of the superlattice. The dotted lines in (d) indicate the directional intermolecular contacts formed by the groups of surfactant chains from facets on neighboring nanocrystals. Taken from Harfenist, S. A.; Wang, Z. L.; Alvarez, M. M.; Vezmar, I.; Whetten, R. L. *J. Phys. Chem.* **1996**, *100*, 13904−13910 (ref 78).

similarly deposited onto electrodes.[72] The success of forming well-ordered 2D arrays and/or 3D networks rests upon the adsorption of truly monodispersed nanoparticles.

Crystallization of suitably derivatized nanoparticles into well-ordered arrays has also been demonstrated.[73−75] Differently sized alkanethiol-derivatized gold nanoparticles, depending on experimental conditions, organized themselves into ordered bimodal arrays, size-segregated regions of hexagonal close-packed monodispersed particles, and random arrangements of pseudohexagonal lattices.[76,55] Of particular significance is the formation of well-characterized size-selected crystalline-thiol-capped gold and silver nanonanoparticles and nanocrystal arrays (see Figure 4, for example).[77−83] Fractional crystallization from toluene by the addition of different amounts of a miscible nondispersing solvent (typically acetone) yielded a series of thiol-capped gold nanoparticles (with Au-core diameters ranging from 1.1 to 3.1 nm) which could be treated (isolated as solid and redispersed in a nonpolar solvent without any structural alteration) and characterized like any large molecules. Significantly, sharp Bragg peaks were observed in the X-ray diffraction of the gold nanoparticle a high degree of ordering into body-centered cubic (bcc), near bcc, or face-centered (fcc) packing.[81]

Self-assembly has also been shown to be mediated by capillary forces,[84,85] temperature control,[86] and dialysis[87] to drive millimeter-scale objects and gold nanoparticles into three-dimensional crystalline arrays.

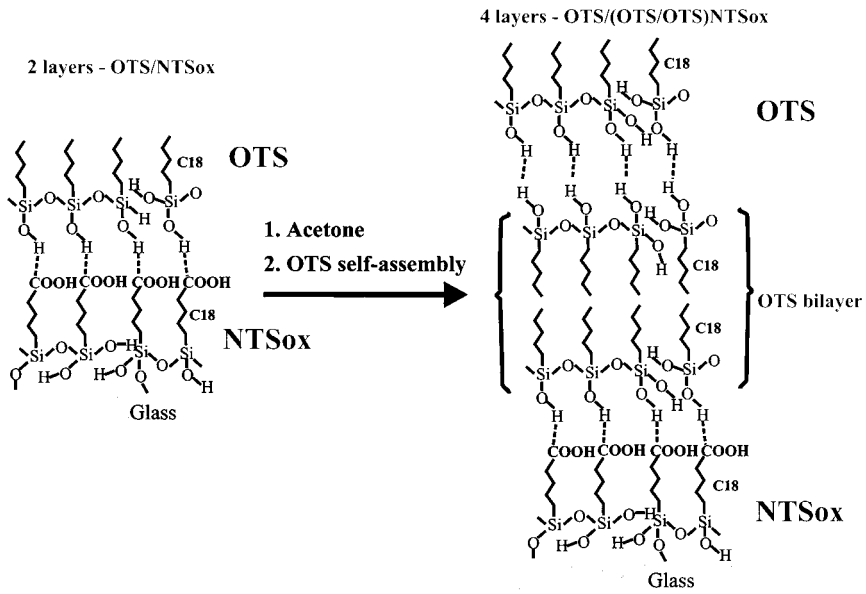

Figure 5. Schematics of "bilayer-within-bilayer" replication of silanes. Taken from Maoz, R.; Sagiv, J. *Adv. Mater.* **1998**, *10*, 580−584 (ref 96).

Capped (derivatized) nanoparticles can be tethered to a substrate to form ordered two-dimensional networks and three-dimensional arrays. Two different approaches have been used. The first (and historically the earlier)[24] approach involved the self-assembly of a bifunctional monolayer onto a substrate (formation of a SAM from an α,ω-dithiol, for example) and then the subsequent attachment of the nanoparticles to the monolayers.[88,89] The second approach involved the derivatization of nanoparticles themselves by bifunctional molecules and their connection subsequently to each other and to substrates.[90,91] Thus, the formation of multilayer films have been reported upon the deposition of 6-nm gold particles, stabilized by α,ω-dithiols onto glass substrates.[90−92] Alternatively, "naked" gold nanoparticles were layer-by-layer self-assembled onto a 3-mercaptopropyl trimethoxysilane derivatized glass (each adsorbed layer of gold nanoparticles was capped by 1,4-benzenedimethanethiol).[93] Formation of self-organized fibrous material was also reported on the decomposition of $AuCl(NH_2R$; R = C_8H_{17}; $C_{12}H_{25}$; $C_{16}H_{33})$ complexes.[94]

An interesting approach to multilayer formation by targeted self-replication of silane multilayers was reported recently.[95,96] Exposure of a self-assembled bilayer of hydrogen-bonded silane and carboxyl-group-terminated silane SAM to undried acetone and immediate immersion into an OTS solution in dried bicyclohexyl led to the insertion of a new silane bilayer (Figure 5). Consecutively repeating the process *n* times produced an identically organized 8 ($n = 2$), 16 ($n = 3$), and 2×2^n layers of film by "bilayer-within-bilayer" intercalation.[96,67]

Advantage has also been taken of the nucleotide base-pair recognition in DNA hybridization for the construction of 2D arrays and 3D networks.[97−103] The approach is illustrated by the hybridization of thiol-functionalized oligonucleotide SAMs with complimentary thiol-functionalized gold nanoparticles to produce a gold substrate−DNA link−gold nanoparticle array (Figure 6). The purpose of adding a thiol spacer (6-mercapto-1-hexanol, for example) is to minimize nonspecific adsorption and to ensure the perpendicular orientation of the thiol-functionalized oligonucleotides.[98] Judiciously mixing the spacer with the thiol-functionalized oligonucleotide provides some control over the distances between the gold nanoparticles, introduced upon hybridization by a thiol-functionalized complementary oligonucleotide (Figure 5). Because having a high pH and heating the DNA duplexes above the melting point result in dehybridization,[104−106] attachment of the gold nanoparticles (through hybridization) is reversible. This reversible hybridization has been exploited for sensor construction.[101]

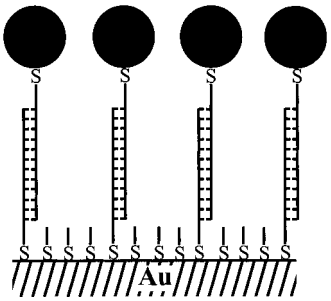

Figure 6. Schematics of a DNA hybridization based self-assembly of gold nanoparticles onto a gold substrate The method involves (i) the formation of a thiol-functionalized oligonucleotide SAM on a gold substrate and (2) its hybridization by a complimentary thiol-functionalized oligonucleotide onto which gold nanoparticles had been attached by S−Au bonding.

Advantage has been taken of well-ordered 2D nanoparticles for substrate patterning.[26] In one approach electron beam exposure is used to etch the substrate between the tightly packed 2D nanoparticle arrays and the subsequent removal of the nanoparticles results in a patterned substrate.[107,108]

II.4. Layer-by-Layer Self-assembly of Ultrathin Films. Self-assembly of alternating layers of oppositely charged polyelectrolytes and nanoparticles (or nanoplatelets) is deceptively simple (see Figure 7). Self-assembly is governed by a delicate balance between adsorption and desorption equilibria. In the self-as-

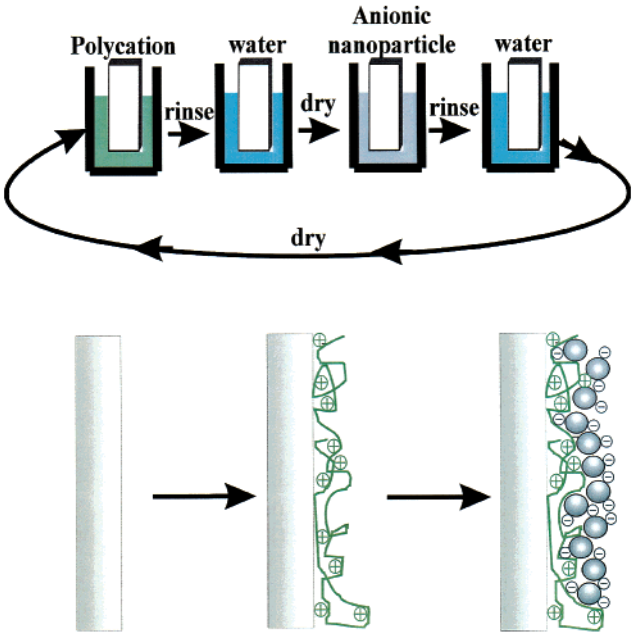

Figure 7. Schematics of spontaneous self-assembly of a nanostructured film. A well-cleaned substrate is immersed into a dilute aqueous cationic polyelectrolyte solution for a time optimized for the adsorption of a 2.0 ± 0.5 nm thick polymer, rinsed, and dried. Next, the polycation-coated substrate is immersed into a dilute dispersion of negatively charged nanoparticles for a time optimized for adsorption of a monoparticulate layer, rinsed, and dried to form an organic–inorganic sandwich unit. Subsequent sandwich units are deposited analogously. The method is amenable to the fabrication of more complex superlattices and scale-up.

sembly of nanoparticles, for example, the efficient adsorption of one (and only one) monoparticulate layer of nanoparticles onto the oppositely charged substrate surface is the objective of the immersion step. Desorption of nanoparticles forming a second and additional layers (and preventing the desorption of the first added layer) is the purpose of the rinsing process. The optimization of the self-assembly in terms of maximizing the adsorption of nanoparticles from their dispersions and minimizing their desorption on rinsing requires the judicious selection of stabilizer(s) and the careful control of the kinetics of the process.

Forces between nanoparticles (or nanoplatelets) and binder nanolayers (polyions or dithiols, for example) govern the spontaneous layer-by-layer self-assembly of ultrathin films. These forces are primarily electrostatic and covalent (for self-assembled monolayers, SAMs, of dithiol derivatives onto metallic surfaces) in nature, but they can also involve hydrogen bonding, $\pi-\pi$ interactions, van der Waals attractions, hydrophobic and epitaxial or other types of interactions. It is important to recognize that polyionic binders must have counterions which can be displaced to electrostatically bind them to the oppositely charged surface. The use of dithiols is only relevant with building blocks which incorporate accessible metal atoms, M (Au and Ag nanoparticles, for example) or semiconducting nanoparticles (MS and MSe, for example where M = Cd, Zn, Pb) in which covalent M–S bonds can be formed. The properties of the self-assembled multilayers depend primarily on the choice of the building blocks used, their rational organization, and integration along the axis perpendicular to the substrate.

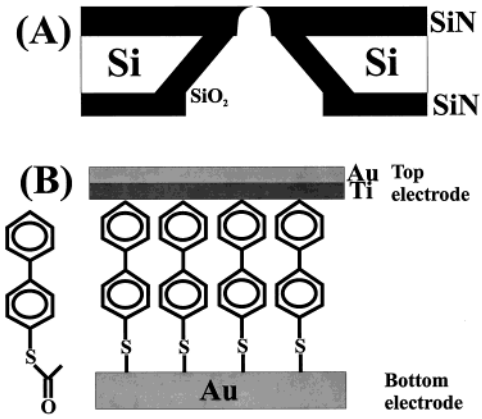

Figure 8. Nanofabricated heterojunction formed by the self-assembly of a 4-thioacetylbiphenyl onto gold (B) evaporated onto the bottom space of a bowl-shaped ca. 300-Å diameter pore formed by electron beam lithography and plasma etching, on a suspended SiN membrane (A). The top electrode is formed by evaporating (in ultrahigh vacuum) titanium (10 Å, followed by 30 Å) and gold (800 Å) onto the SAM, at a very low deposition rate (0.3 Å/s) and at low temperatures. Taken from Zhou, C.; Deshpande, M. R.; Reed, M. A.; Jones, L.; Tour, J. M. *Appl. Phys. Lett.* **1997**, *71*, 611–613 (ref 124).

Sequential adsorption of oppositely charged colloids was reported in a seminal paper.[109] Self-assembly was subsequently "rediscovered" and extended to the preparation of multilayers of polycations and phosphonate anions[110–113] and to the layering of polyelectrolyte.[101] Construction of electrodes coated by polyelectrolytes, clays, and other materials often involved self-assembly,[114,115] albeit the method had not been called as such. Self-assembly is now routinely employed for the fabrication of ultrathin films from charged nanoparticles (metallic, semiconducting, magnetic, ferroelectric, and insulating, for example), nanoplatelets (clays or graphite platelets, for example), proteins, pigments, and other supramolecular species.[113,116–118] Indeed, layer-by-layer self-assembly has been recognized as a subfield of colloid chemistry and the exponentially increasing research publications are listed at a website.[119]

That a large variety of molecules, polyelectrolytes, nanoparticles, and nanoplatelets can be layer-by-layer adsorbed, in any desired order, is the greatest advantage of self-assembly. The oppositely charged species are held together by strong ionic bonds and form long-lasting, uniform, and stable films which are often impervious to solvents. No special film balance is required for the self-assembly; indeed, the method has been referred to as a "Molecular Beaker Epitaxy".[120] Furthermore, self-assembly is economical (dilute solutions and dispersions are used and the materials can be recovered) and readily amenable to scaling-up for the fabrication of large-area defect-free devices on virtually any kind and shape of surfaces.

III. Examples of Potential Electronic Applications

Careful manipulation of the chemical structure of the molecules constituting the SAM permits the construction of fully conducting, completely isolating, or semiconducting ultrathin films on metal surfaces. Suitably selected SAMs can also change the Schottky energy barrier in a heterojunction by functioning as an oriented

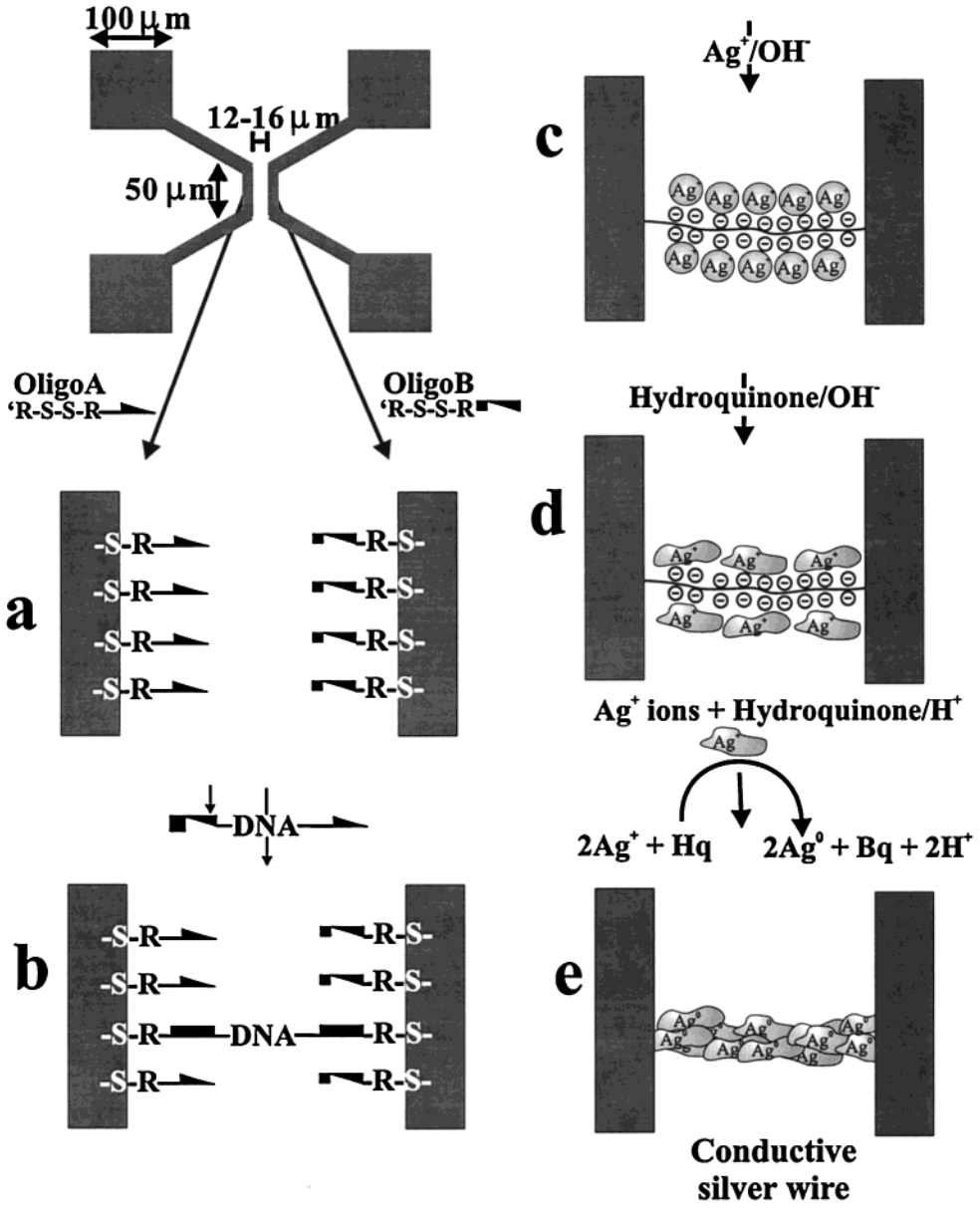

Figure 9. Fabrication of a silver nanowire connecting two gold electrodes (top left). (a) One gold electrode was wetted with a droplet of 0.2 nM 5′-GGGCGGCGACCT-3′-disulfide oligonucleotide (oligo A) and 10 nM NaCl. The other electrode was similarly treated by AGGTCGCCGCCC-3′-disulfide oligonucleotide (oligo B). (b) After rinsing, the electrode was covered by a 0.2 pM solution of λ-DNA which had two sticky ends, complimentary to oligo A and oligo B. A flow of solution perpendicular to the electrodes stretched the λ-DNA molecules, leading to hybridization. (c) The DNA was loaded by silver ions by immersion into 0.1 M $AgNO_3$ and **(**d) complexed by the addition 0.05 M NH_4OH. (e) The DNA-templated wire was developed by the reduction of DNA-bound Ag^+ to silver metal by 0.05 M hydroquinone in the presence of citrate buffer (pH = 3.5). Taken from Braun, E.; Eichen, Y.; Sivan, U.; Ben-Yoseph, G. *Nature* **1998**, *391*, 775−778 (ref 129).

dipole layer. Thus, for example, hole injection from a copper electrode into a layer of conjugated polymer was found either to improve or to degrade upon the self-assembly of a monolayer of either $HS(C_6H_4C_2)_2C_6H_4-F$ or $HS(C_6H_4C_2)_2C_6H_4-H$, respectively, between this junction.[121] The effect of SAMs originates in the changing of the surface potential of the copper electrode. When the Kelvin probe technique (i.e., making the current zero between a vibrating Kelvin probe tip and the substrate surface by an applied bias voltage to define the surface potential between the substrate and the tip) was used, a surface potential change of +0.3 V and −0.2 V was determined for the $HS(C_6H_4C_2)_2C_6H_4-F$ and $HS(C_6H_4C_2)_2C_6H_4-H$ SAM-coated copper electrode with respect to the uncoated electrode.[121]

The beneficial properties of SAMs can be fruitfully exploited in potential nanoelectronic applications.[122] Creating a metal/SAM/metal junction and/or connecting a wire to the SAM remain, however, a formidable challenge. Evaporation of a metal (aluminum or gold, for example) layer onto or the use of silver paints on the SAM may well damage the monolayer and cause electrical shorting. Attempts to overcome this problem included the construction of more complex self-assembled films (10 or more layer-by-layer self-assembled polyelectrolytes, nanoparticles, and/or depositing a semiconducting polymer under and/or onto the self-assembled layers),[123] the nanofabrication of special junctions (Figure 8, for example),[124,125] the design of nanowires[126−128] (see Figure 9, for example),[129] and the

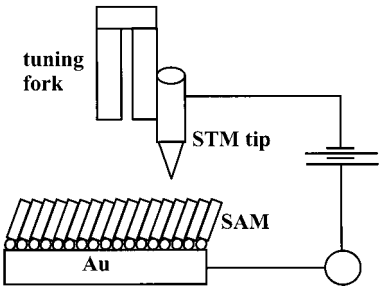

Figure 10. Schematics of a tuning fork based SPM capable of rapid $i-V$ measurements of SAMs. Taken from Fan, F. R. F.; Yang, J. P.; Dirk, S. M.; Price, D. W.; Kosynkin, D.; Tour, J. M.; Bard, A. J. *J. Am. Chem. Soc.* **2001**, *123*, 2454−2455 (ref 132).

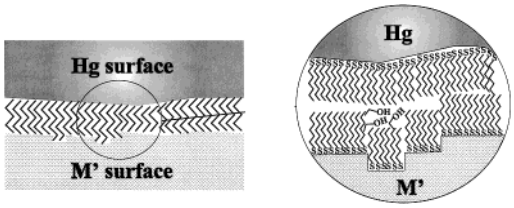

Figure 11. Schematic representation of a Hg-SAM/SAM-metal junction. The liquid Hg-SAM surface comes into conformational contact with the SAM-metal surface. The uniformity of the contact at the atomic level is unclear; indeed, the presence of solvent (ethanol) between the SAM layers is indicated. Taken from Haag, R.; Rampi, M. A.; Holmlin, R. E.; Whitesides, G. M. *J. Am. Chem. Soc.* **1999**, *121*, 7895−7906 (ref 133).

examination of single-electron-transfer events by AFM (where electrical contact is made between a conducting AFM tip and an isolated MPC, tethered to a conducting substrate, for example).[130,131] Of importance is the recently reported rapid electrical characterization of SAMs by a tuning fork based scanning probe microscope (Figure 10).[132]

Examples will be provided for the formation junctions, heterojunction, and single-electron transfer in the subsequent sections.

III.1. Metal/SAM Junctions. Examination of metal/SAM/metal junctions in the solid state, as stated above, is plagued by the damage of the SAM and electrical shorting. Valuable information has been obtained, however, by measuring electrical breakdown voltages, BDVs, in a recently proposed relatively simple and experimentally flexible Hg-SAM/SAM-metal junction (Figure 11).[133] The measured values for BDVs were found to increase with increasing packing density and decreasing tilt angle of the SAM constituting thiols. Furthermore, SAMs composed of C14 or longer chain length alkane thiols sustained a constant electrical field up to $8 \pm 1 \times 10^8$ V/m on silver substrates, a performance similar to that of a micrometer-thick polyethylene.[133]

Electrochemical examination of SAMs, deposited onto electrodes in aqueous solutions, should also be mentioned. Cyclic voltammetry, electrical impedance spectroscopy, and chronoamerometry (of aqueous solutions of the $[Fe(CN)_6]^{3-}/[Fe(CN)_6]^{4-}$ redox couple as well as electroactive SAMs) provided information on the substrate metal coverage by the SAMs and, more importantly, permitted the determination of electron tunneling from redox centers, attached or adsorbed onto the SAM, to the electrode (or *vice versa*). Significantly, the determined electron-transfer rate constants and reorganization energies were found to be in good agreement with theoretical predictions.[134−136] The junctions investigated produced a diode-like response[137] and allowed the quantitative examination of charge-transfer processes in SAMS.[138] These results have opened the door, in turn, to the meaningful design of sensors[139] and photelectrochemical solar energy converting systems.[140−142]

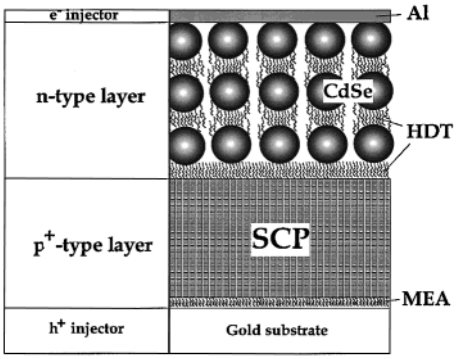

Figure 12. Fabrication of a p^+-n junction capable to function as a rectifying device undergoing a Zener breakdown. The device consists of two layers: the first layer is a p-doped semiconductor polymer, SCP (polypyrrole, Ppy^+, for example), deposited onto a pretreated (by mercaptoethylamine hydrochloride, MEA) conducting substrate (gold, for example) which serves as the anode. The second layer is composed of n-type semiconductor nanoparticles (cadmium selenide, CdSe, for example) and 1,6-hexanediol, HDT, layer-by-layer self-assembled onto the first layer and coated by a thin film of aluminum (Al) which serves as the cathode. Taken from reference Cassagneau, T.; Mallouk, T. E.; Fendler, J. H. *J. Am. Chem. Soc.* **1998**, *120*, 7848−7859 (ref 144).

III.2. More Complex Heterojunctions. Rectifying behavior for layer-by-layer self-assembled films with total thickness on the order of 6 nm (or less) has been observed in specially fabricated heterostructures (see Figure 8, for example) in the solid state.[124,143]

Rectification could be demonstrated on a more complex and thicker (on the order of 20 nm or more) self-assembled films using standard electrical measurements. We have reported, for example, the construction of a ultrathin rectifying heterojunction by chemical assembly and self-assembly.[144] Ultrathin films were prepared by self-assembling trioctylphosphine oxide, TOPO, capped n-type 20−40-Å diameter CdSe nanoparticles and 1,6-hexadecanethiol, HDT, onto p-doped semiconducting polymers, SCP (electrochemically deposited poly(3-methylthiophene), PMeT, or chemically deposited poly(pyrrole), Ppy). The SCP was formed on a mercaptoethylamnie (MEA) pretreated gold substrate. Electrical contact was made by connecting the gold substrate to aluminum, evaporated onto the CdSe nanoparticles (Figure 12). Electrical properties of these heterojunctions were characterized by current (i) voltage (V) measurements. The $i-V$ characteristics manifested themselves in a forward and a reverse branch (Figures 13). Injection of charges was believed to occur mainly by tunneling through the interfaces between the electrodes and the hole or electron conductors. The observed tunneling mechanism can be expressed by the Fowler−

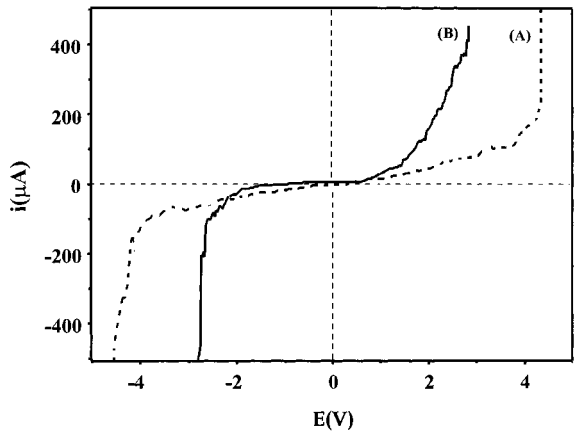

Figure 13. *i*−*V* characteristics measured for an Au/p-doped PMeT film/(Al_2O_3)-Al (A) and for an Au/p-doped PMeT film/(HDT/CdSe)$_3$/(Al_2O_3)-Al (B). Taken from Cassagneau, T.; Mallouk, T. E.; Fendler, J. H. *J. Am. Chem. Soc.* **1998**, *120*, 7848−7859 (ref 144).

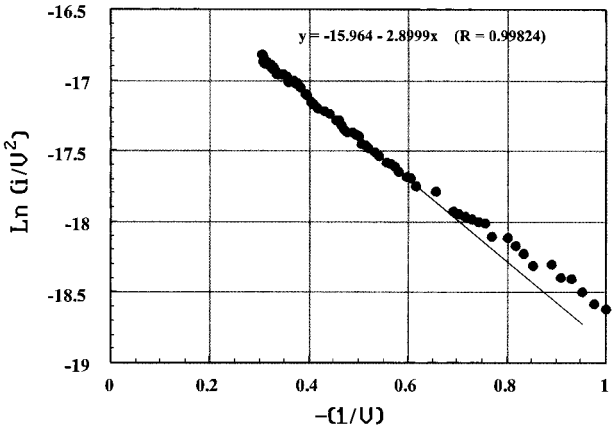

Figure 14. Fowler−Nordheim plot calculated from the *i*−*V* characteristic of the system Au/p-doped PMeT film/(HDT/CdSe)$_3$/(Al_2O_3)-Al in the forward direction. Taken from Cassagneau, T.; Mallouk, T. E.; Fendler, J. H. *J. Am. Chem. Soc.* **1998**, *120*, 7848−7859 (ref 144).

Nordheim equation which describes the field emission tunneling current, *I*, as a function of the bias voltage:[145]

$$I = V^2 \exp(-\beta d/V) \qquad (2)$$

where *d* is the thickness of the device sandwiched between the electrodes. Plotting eq 1 logarithmically led to a good straight line (Figure 14) which permitted the fitting of the forward branch of the *i*−*V* curve. The reverse branch did not follow either a Schottky or a Fowler−Nordheim law but indicated a Zener breakdown.

The Zener breakdown should appear at a potential which corresponds to the difference between the conduction band edge of CdSe and the valence band edge of the polymer. According to the energy level diagram sketched in Figure 15,[144] this difference is between 2.3 and 2.4 eV at the PMeT$^+$/CdSe junction and about 2.66 eV at the Ppy$^+$/CdSe junction. It is observed that the breakdown occurs at about −2.5 and −2.3 V for PMeT$^+$ and Ppy$^+$, respectively. Thus, the energy required for inducing a reverse current is in fair agreement with the minimum energy to be applied. Therefore, the Zener breakdown is the consequence of the high density of

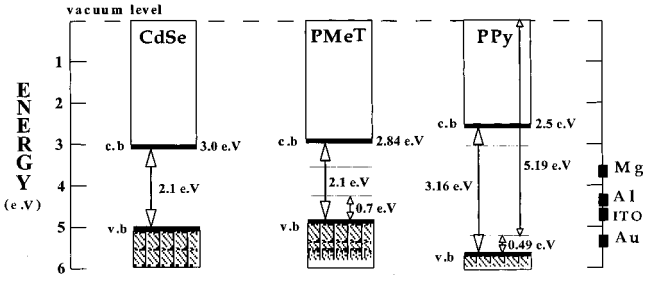

Figure 15. Schematic energy level diagram for a p$^+$-n junction consisting of a p-doped semiconductor polymer (poly(pyrrole), Ppy, or poly(3-methylthiophene), PMeT), and CdSe nanoparticles. Taken from Cassagneau, T.; Mallouk, T. E.; Fendler, J. H. *J. Am. Chem. Soc.* **1998**, *120*, 7848−7859 (ref 144).

donors in the polymer film. The main interest in Zener breakdown is to produce "hot" electrons in the *n*-type layer which could be used, for instance, for stimulating the luminescence in a phosphor and hence to provide a route to bimodal electroluminescence, with two distinguishable emissions depending on the direction of the applied potential.

Ultrathin silicon wafer−silicon nanoparticle junctions were also constructed by chemical assembly and self-assembly (Figure 16).[146] Our method involved the preparation of colloidal 1−10-nm diameter silicon nanocrystallites, Si-nc, by the sonication of anodically etched silicon wafers in toluene and their covalent attachment to derivatized silicon wafers (p-Si-D or n-Si-D). The substrate derivatization consisted of three steps: (i) self-assembly of dimethyloctadecylmethoxysilane (DOMS) onto given substrates, followed by (ii) bromination (iii) and subsequent hydroxylation of the brominated terminal methyl groups to give 18-hydroxydimethyloctadecylsiloxane monolayers covalently attached to the silicon wafers, p-Si-D or n-Si-D. It should be noted, in passing, that we could attach Si-nc to any substrate (gold, glass, and quartz, for example) which can be functionalized by OH groups.[146]

When p-type substrates (p-Si, p-PS, and p-Si-D) were used, the forward bias condition corresponded to the application of a negative voltage to the Ppy film with respect to the back contact on the Si substrate. For the simple p-Si/Ppy/Au junction, the *i*−*V* plot was almost symmetrical. The observed rectification in the p-PS/Ppy/Au films originated in the interface between the PS and the p-Si substrate which behaved like an n-type silicon. Consequently, a p−n-like junction was formed with the bulk p-Si (under the PS layer). The rectification observed with the p-Si-D/n-Si-nc/Ppy/Au junction was caused by the p-Si-D/n-Si-nc interface while the Ppy film assisted the Si-nc in the electron injection.[146]

Interestingly, (p- or n-)Si-D/Si-nc/Ppy/Au junctions were not regulated by the thermionic emission beyond an applied forward bias of 1 V. However, a good fit was found on using the Fowler−Nordheim law (eq 2). At forward bias, electrons are injected into the conduction band of the quantized Si-nc at the cathode (via the Ppy layer), while holes flow along the valence band of the p-doped Si substrate at the anode. Therefore, rectification occurs at the p-Si/Si-nc interface. It should be noted that the reactivity and/or the electronic properties of Si-nc made from p-Si and n-Si were observed to be different in these devices. Specifically, the asymmetry ratio was

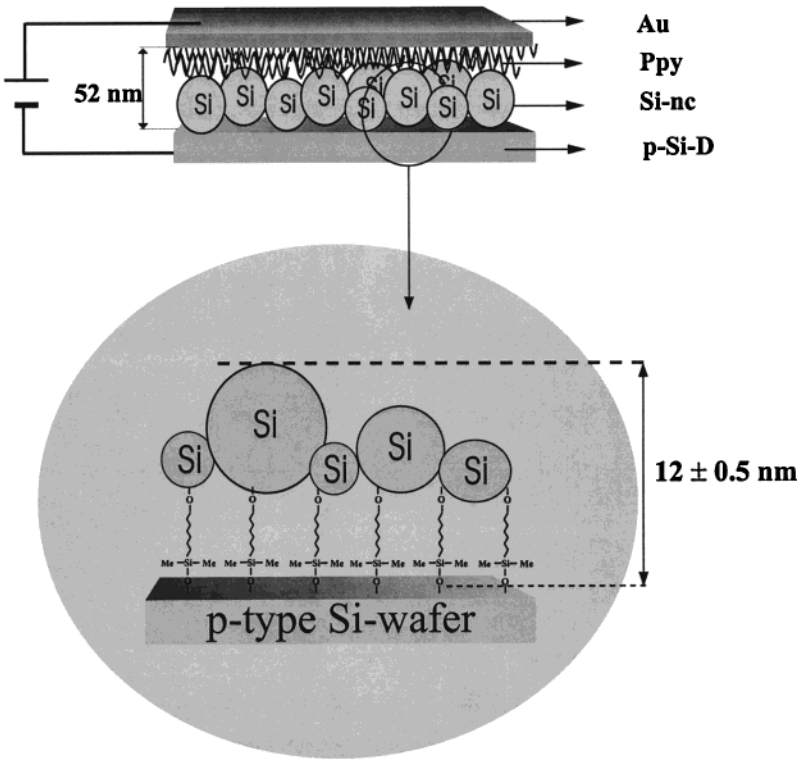

Figure 16. Cross-sectional view of the self-assembled p-D/Si-nc/Ppy/Au junction self-assembled. Taken from Sweryda-Krawiec, B.; Cassagneau, T.; Fendler, J. H. *Adv. Mater.* **1999**, *11*, 659−664 (ref 146).

higher while the current density was lower for Si-nc obtained from p-Si than those prepared from n-Si. These differences suggest that sizes, size distributions, surface defects, and reactivity toward the OH-terminated monolayer of Si-nc play an important role in the properties of the junctions constructed.[146] Reversing the bias led to the injection of electrons into the conduction band of p-Si and their rapid recombination with the holes already present in the valence band (see curves c and d in Figure 17A). Size-quantized Si-nc at the p-Si-D/Ppy interface dramatically improved the rectifying properties of the junctions (compare curves b and d in Figure 17A). The conduction band shifts upward about half as much as the downward shift of the valence band in Si-nc up size quantization, which is negligible for Si particles larger than 5 nm. The conduction band edge of Si-nc is located at almost the same level as the conduction band edge of PS. This may explain why both the p-PS/Ppy/Au and p-Si-D/Si-nc/Ppy/Au film were rectifying at forward bias. It also justifies this method of construction of electroactive junctions by the layer-by-layer self-assembly of silicon nanocrystallites.[146]

n-Type substrates in n-Si/Ppy/Au, n-Si-D/Si-nc/Ppy/Au, and n-Si-D/Si-nc/Au films were also tested. For these films, the polarity of the back contact electrode was made negative relative to the gold contact, under a forward bias. The n-Si/Ppy/Au (see curve f in Figure 17B) and n-Si-D/Si-nc/Au junctions (not shown) did not exhibit rectification at +2 V and the current was negligible. Introducing a layer of Si-nc (made from etching of n-Si) between n-Si-D and Ppy (n-Si-D/Si-nc/Ppy/Au) led to a dramatic change in the $i-V$ curve (see curve h in Figure 15B). An asymmetry ratio of 138 was found, with the highest current densities determined (490 μA/cm^2 at +2 V). The valence band edge of size-quantized Si-nc can be located at lower energy (5.5 eV and below) than that of Ppy (5.7 eV) thereby favoring hole injection, while the valence band edge of PS (6.2 eV) is at much higher energy. The meager rectification in the n-PS/Ppy/Au film (curve g in Figure 17B) at forward bias, in contrast to pronounced rectification on employing size-quantized Si-nc at the interface n-Si-D/Si-nc (curve h in Figure 15B), is rationalized analogously. As expected, the barrier height to overcome tunneling was observed to increase proportionally to the current density at a given voltage, that is, +2 V.[146]

Interfacial electron transfer has been shown to be controlled by the charge (positive or negative) on the outermost polyelectrolyte in layer-by-layer self-assembled films.[147] Negatively charged poly(acrylic acid) and positively charged polylysine were layer-by-layer self-assembled onto a cystamine SAM functionalized gold working electrode. Efficient electron transfer from the $[Fe(CN)_6]^{3-}/[Fe(CN)_6]^{4-}$ redox couple (in aqueous solution, using a conventional three-electrode cell) was only possible if positively charged polylysine was the outermost layer on the working electrode. Self-assembled films terminating in negatively charged poly(acrilic acid) showed high resistance to electron transfer. Apparently, electron transfer was found to be governed by electrostatic interactions at the coated electrode electrolyte interface while the porous structure of the self-assembled polyelectrolyte film allowed redox transformations (with nonlinear decrease with increasing thickness of the polyelectrolyte layers self-assembled) at the electrode surface.[147] Similarly constructed electrodes have been demonstrated to function as sensors,[148−152] signal transducers,[153] molecular transporters,[154,155] and photoelectrochemical solar cells.[156,157]

III.3. Single-Electron Transfer. Single-electron conductivity implies, by definition, the controllable charge transport by individual electrons. There are two

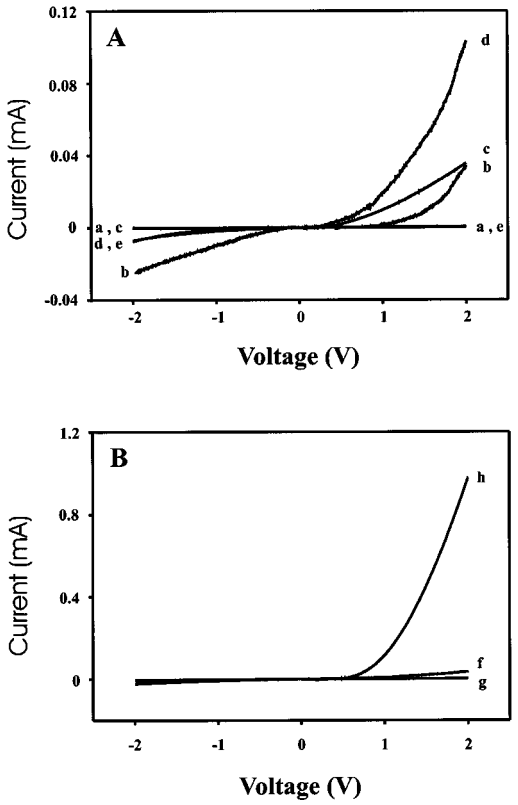

Figure 17. Electrical characteristics of the different junctions investigated: A = all devices with a back contact to p-type silicon wafers polarized positively under a forward bias. a = p-Si/Ppy/Au; b = p-PS/Ppy/Au; c = p-Si-D/Si-nc (prepared from p-Si)/Ppy/Au; d = p-Si-D/Si-nc (prepared from n-Si)/Ppy/Au; e = p-Si-D/Si-nc (prepared from p-Si)/Au. B = all devices with back contact polarized negatively under a forward bias. f = n-Si/Ppy/Au; g = n-PS/Ppy/Au; h = n-Si-D/Si-nc (prepared from n-Si)/Ppy/Au. Taken from Sweryda-Krawiec, B.; Cassagneau, T.; Fendler, J. H. *Adv. Mater.* **1999**, *11*, 659−664 (ref 146).

stringent requirements for the observation of single-electron events. First, the electrostatic energy of introducing an electron into an isolated conductor, E_c, has to be larger than its thermal fluctuation, k_BT:

$$E_c = e^2/2C \gg k_BT \qquad (3)$$

(where C is the effective capacitance of the conductor, e is the charge of the electron, k_B is the Boltzmann constant, and T is the absolute temperature). This can be accomplished by decreasing the temperature or the capacitance or, indeed, decreasing both of these parameters. The capacitance is determined by the size of the conductor and its distance from the surrounding electrodes (gates). A simple calculation shows that charging a macroscopic capacitor (having capacitance in the 10^{-12} F range) by a single electron would require a potential of 10^{-8} V and a temperature in the milli-Kelvin range to avoid thermal fluctuations. Single-electron events become observable at room temperatures, however, if the junction capacitance is lowered to the 10^{-18} to 10^{-19} F range. This can be best achieved by entrapping a conducting nanoparticle (with a diameter <2 nm) into an appropriate tunneling barrier[158] or by placing a highly ordered and closely packed monodispersed (σ < 10%) array of conducting nanoparticles (with diameters <2 nm, each of which are protected by an insulating surfactant monolayer) between macroscopic electrodes.[159−161]

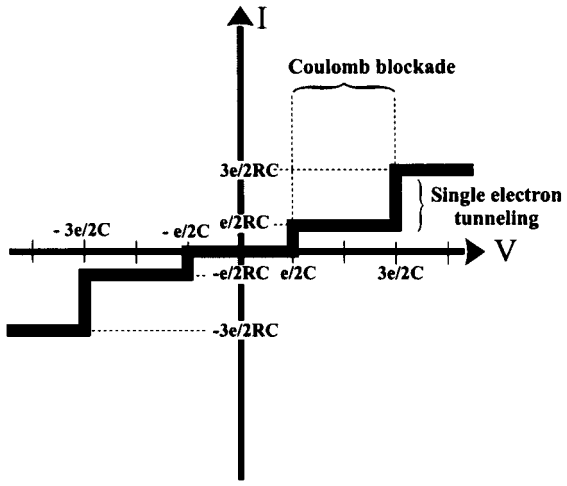

Figure 18. Ideal staircase $i-V$ characteristics of a single-electron tunneling junction. As the junction is biased by a constant current I, at $|Q| > e/2$, a tunneling event takes place, making $|Q|$ jump to $-e/2$ and a new charging cycle restarts. The junction is Coulomb blockaded as long as $|Q| < e/2$ or the voltage $V < e/2C$ (plateau of the current), while single-electron tunneling is characterized by a jump of the current at $|Q| > e/2$. Because the current is proportional to the reciprocal of the resistance R of the junction times the voltage, each single-electron tunneling generates a jump of e/RC in the current.

The second requirement for realizing single-electron events is that the dielectric constant of the barrier which surrounds the conducting nanoparticle should have a tunneling resistance, R_T, which exceeds the resistance quantum, R_Q ($R_T \gg R_Q$, $R_Q = h/e^2 \approx 25.8$ kΩ). This requirement can be met by selecting an insulating barrier which ensures the localization of the electron in (or on) the nanoparticle.

Single-electron trapping and flow manifest themselves in an observable Coulomb blockade, Coulomb staircase, and differential negative resistance in contrast to the classical ohmic behavior of a macroscopic capacitance device. Thus, application of a bias voltage of $e/2C$ (or an odd multiple of $e/2C$) to the monolayer-protected nanoparticle (by the conducting tip of the AFM, for example) is required for the current to flow through the circuit. When the charge, $|Q|$, on the junction is smaller than $e/2$ ($|Q| < e/2$), the potential energy barrier of the trapped single electron, already present in (or on) the nanoparticle, cannot be overcome; that is to say the entry of the next incoming electron is Coulomb Blockaded. When the junction is biased at a constant current, I, at $|Q| > e/2$, electrons will tunnel in increments with a frequency of I/e. The incremental electron tunneling manifests itself in the appearance of steps in the current−voltage plots, that is, in the setup of a Coulomb Staircase (Figure 18). Oscillations at the steps in the current−voltage plots sometimes become also observable as differential negative resistance regions. For single-electron transport, there is a linear relationship between the current and the frequency of the voltage signal. Superimposing a sinusoidal signal onto the bias voltage, the amplitude of the measured current through the conducting nanoparticle is proportional to the signal frequency. Furthermore, the ratio of the current to the frequency is equal to the electron charge.

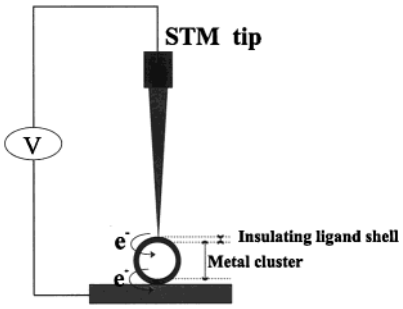

Figure 19. Schematic representation of a tunneling junction made upon applying a voltage between a ligand-stabilized metal cluster and a STM tip. Both the tip and the substrate are conductive and the ligand shell is the tunneling barrier between these two electrodes and the metallic core of the cluster.

Single-electron tunneling, at low temperatures, has been observed by scanning tunneling microscopy.[158] Evidence has been obtained for Coulomb staircase behavior, for example, on charging a 1,10-phenantroline ligand (phen) stabilized 2.1-nm diameter platinum cluster, $Pt_{309}phen_{36}O_{20}$, by an STM tip, on a gold substrate at 4.2 K (Figure 19).[162] Single-electron-transfer events have been observed at room temperature in polymer spin-coated (35-nm-thick poly(methyl methacrylate), PMMA) highly ordered arrays of 2−4-nm diameter silver nanoparticles between Al electrodes,[163] in CdS nanoparticles, in situ generated on conducting AFM tips,[164] in gold nanoparticles connected by dithiol SAMs to a gold substrate,[158,165] in gold nanoparticles incorporated into a source-drain-gate nanofabricated device,[166,167] and in organized and surface capped gold nanoparticles.[168]

Particularly interesting is the recently observed single-electron transfers in monolayer-protected gold cluster dispersions by differential pulse voltammetry; these experiments have been likened to "doing redox chemistry with quantum capacitors"[57,169] observing "quantized double-layer charging".[53] Because the magnitude of the capacitance on an MPC is on the order of 10^{-18} to 10^{-19}(atto−subatto) F range, charging of a single particle occurs in potential intervals (described by eq 2) which can be observed in voltammetry. Indeed, this has been reported for gold MPCs.[57,170−182] Using controlled potentials permitted the estimation of the average number of electrons stored on the MPCs from the pattern of voltammograms. Single-electron transfer involving MPCs is analogous then to the Coulomb staircase, albeit requiring a different equivalent circuit (Figure 20).[53,172] More recently, quantized double-layer charge of gold MPCc, immobilized onto gold substrates by SAM, has also been demonstrated.[173,174]

Three-dimensionally size-quantized semiconductor nanoparticles (quantum dots) is often referred to as artificial atoms by the physicists because their electronic wave functions are predicted to exhibit atomic-like symmetries.[175−181] Indeed, discrete energy level structures have ben reported for many size-quantized semiconductor nanoparticles.[6] The concept of artificial atoms should stimulate the development of new theories and quantum dot based computing and devices.

To the best of our knowledge, there is only one published report on single-electron charging of a layer-by-layer self-assembled ultrathin film.[182] Sequential

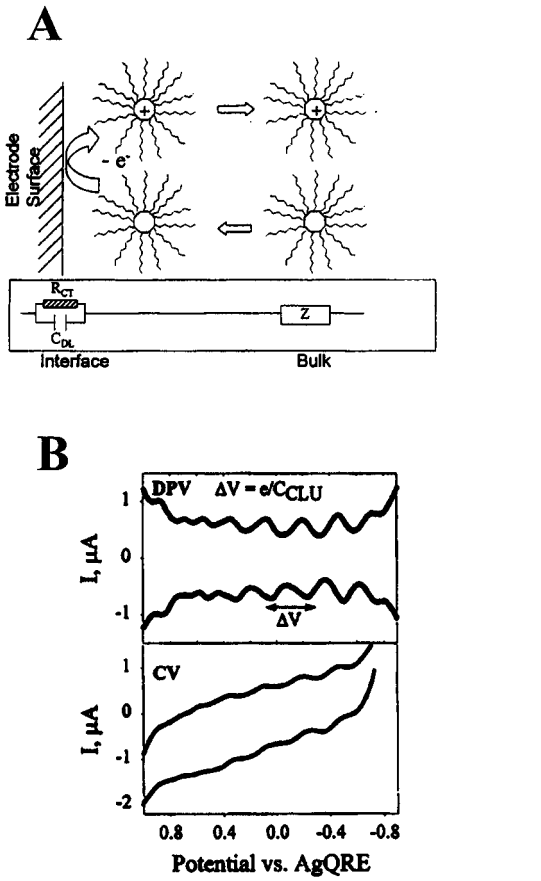

Figure 20. A = A cartoon of quantized double-layer charging of neutral MPCs diffusing from bulk solution to an electrode/solution interface charged with a potential $E_{PZC} \pm e/C_{CLU}$. All MPCs are charged to that potential by ± a single electron and then diffuse back to the solution. B = differential pulse voltammetry (top) and cyclic voltammetry (bottom) of hexanethiolate gold MPC. Taken from Templeton, A. C.; Wuelfing, M. P.; Murray, R. W. *Acc. Chem. Res.* **2000**, *33*, 27−36 (ref 53).

self-assembly of anionic exfoliated zirconium phosphate, α-$Zr(HPO_4)_2H_2O$ (α-ZrP), poly(allylamine hydrochloride) (PAH), negatively charged gold nanoparticles (Au), PAH, α-ZrP, and poly(pyrrole) (Ppy) onto a mercaptoethylamine hydrochloride (MEA) treated gold substrate leads to the formation of a metal−insulator−gold nanoparticle−insulator−metal, MINIM ultrathin film, Au-MEA/α-ZrP/PAH/Au/PAH/α-ZrP/PPy. Current−voltage curves of this MINIM device displayed tunable Coulomb gaps.[182]

These investigations have been largely motivated by the perceived possibility of constructing a memory storage device based on the presence or the absence of a single electron on a nanoparticle. Furthermore, understanding the behavior of individual nanoparticles (which we have learned to treat as if they were molecules) and their collective ensemble will aid the transition to molecular electronics.[183−187] Fabrication of single-electron transistors will also open the door to a large variety of nanoelectronic applications.

IV. Conclusion

These are exciting times for chemists. Inspired by biomineralization, they can apply their expertise to

assembly and preside over the self-assembly of 2D and 3D structures on the nanometer scale from a large variety of chemicals. Taking advantage of established chemistries, they can select molecules and clusters of molecules which function as insulators, semiconductors, conductors, and even superconductors and have a vast range of desirable properties. Indeed, metallic, semiconducting, magnetic, and ferroelectric nanoparticles have been prepared and chemical self-assembly has been demonstrated to produce, in addition to the electronic application highlighted here, optical, electro-optical, charge, and memory storage devices. We are only at the beginning of the chemical approach to advanced materials preparation and can confidently look forward to the unexpected and unthought of discoveries.

References

(1) Mann, S. *Mineralization in biological systems*; Clarke, M. J., Goodenough, J. B., Ibers, J. A., Jorgensen, C. K., Neilands, J. B., Reinen, D., Weiss, R., Williams, R. J. P., Eds.; Springer-Verlag: Berlin, 1983; pp 125−174.
(2) Addadi, L.; Weiner, S. *Angew. Chem.* **1991**, *31*, 153−169.
(3) Levi, Y.; Albeck, S.; Brack, A.; Weiner, S.; Addadi, L. *Chem.-Eur. J.* **1998**, *4*, 389−396.
(4) Viney, C. *Natural Silks—Archetypal Supramolecular Assembly of Polymer Fibers*; Viney, C., Ed.; Elsevier Sci Ltd: Oxford, 1997; pp 75−81.
(5) Bazylinski, D. A.; Garratt-Reed, A. J.; Frankel, R. B. *Microsc. Res. Tech.* **1994**, *27*, 389−401.
(6) Fendler, J. H. *Membrane Mimetic Approach to Advanced Materials*; Springer-Verlag: Berlin, 1992; Vol. 113.
(7) Mann, S. *Biomimetic Materials Chemistry*; VCH: New York, 1996.
(8) Tirrell, M.; Texter, J. *Materials Design and Processing at the Nano- and Mesoscales Through Self-assembly, Report of the NSF Workshop in Minnesota*; National Science Foundation: Washington, D.C., 1998, Issued October 2000.
(9) Fendler, J. H. *Membrane Mimetic Chemistry, Characterizations and Applications of Micelles, Microemulsions, Monolayers, Bilayers, Vesicles, Host−Guest Systems and Polyions*; John Wiley: New York, 1982.
(10) Blodgett, K. B.; Langmuir, I. *Phys. Rev.* **1937**, *51*, 964−982.
(11) Gaines, G. L. *Insoluble Monolayers at Liquid−Gas Interfaces*; Interscience: New York, 1966.
(12) Ulman, A. *An Introduction to Ultrathin Organic Films from Langmuir Blodgett to Self-Assembly*; Academic Press: Boston, 1991.
(13) Carey, R. I.; Folkers, J. P.; Whitesides, G. M. *Langmuir* **1994**, *10*, 2228−2234.
(14) Ulman, A. *Chem. Rev.* **1996**, *96*, 1533−1554.
(15) Spange, S.; Eismann, U.; Hohne, S.; Langhammer, E. *Application of Cationic Polymerization to Grafting and Coating of Silica Particles*; Spange, S., Eismann, U., Hohne, S., Langhammer, E., Eds.; Huthig & Wepf Verlag: Basel, Switzerland, 1998; pp 223−236.
(16) Hepel, M. *Electrode−Solution Interface Studied with Electrochemical Quartz Crystal Nanobalance*, 1st ed.; Wieckowski, A., Ed.; Marcel Dekker: New York, 1999; Vol. 1, pp 599−630.
(17) Bard, A. J.; Faulkner, L. R. *Electrochemical Methods Fundamentals and Applications*; John Wiley & Sons: New York, 2001; Vol. 1.
(18) Meuse, C. W. *Langmuir* **2000**, *16*, 9483−9487.
(19) Brockman, J. M.; Nelson, B. P.; Corn, R. M. *Annu. Rev. Phys. Chem.* **2000**, *51*, 41−63.
(20) Mendelsohn, R.; Brauner, J. W.; Gericke, A. *Annu. Rev. Phys. Chem.* **1995**, *46*, 305−334.
(21) Wang, Z. L. *Characterization of Nanophase Materials*, 1st ed.; Wang, Z. L., Ed.; Wiley-VCH: Weinheim, Germany, 2000; Vol. 1, p 406.
(22) Pomerantz, M.; Segmüller, A.; Netzer, L.; Sagiv, J. *Thin Solid Films* **1985**, *132*, 153−162.
(23) Vuillaume, D.; Boulas, C.; Collet, J.; Allan, G.; Delerue, C. *Phys. Rev. B: Condens. Matter* **1998**, *58*, 16491−16498.
(24) Sagiv, J. *J. Am. Chem. Soc.* **1980**, *102*, 92−98.
(25) Sagiv, J. *Israel J. Chem.* **1979**, *18*, 339−345.
(26) Xia, Y. N.; Whitesides, G. M. *Annu. Rev. Mater. Sci.* **1998**, *28*, 153−184.
(27) Bain, C. D.; Whitesides, G. M. *J. Am. Chem. Soc.* **1988**, *110*, 3665−3666.
(28) Laibinis, P. E.; Whitesides, G. M.; Allara, D. L.; Tao, Y.-T.; Parikh, A. N.; Nuzzo, R. G. *J. Am. Chem. Soc.* **1991**, *113*, 7152−7167.
(29) Kang, J. F.; Ulman, A.; Liao, S.; Jordan, R.; Yang, G. H.; Liu, G. Y. *Langmuir* **2001**, *17*, 95−106.
(30) Fendler, J. H.. *Membrane-Mimetic Approach to Advanced Materials*; Springer-Verlag: Berlin, 1994; p 1.
(31) Bishop, A. R.; Nuzzo, R. G. *Curr. Opin. Colloid Interface Sci.* **1996**, *1*, 127−136.
(32) Schreiber, F. *Prog. Surf. Sci.* **2000**, *65*, 151−256.
(33) Porter, M. D.; Bright, T. B.; Allara, D. L.; Chidsey, C. E. D. *J. Am. Chem. Soc.* **1987**, *109*, 3559−3568.
(34) Wang, J.; Jiang, M.; Kawde, A. M.; Polsky, R. *Langmuir* **2000**, *16*, 9687−9689.
(35) Evans, D. F.; Wennerstrom, H. *The Colloid Domain. Where Physics, Chemistry and Technology Meet*; VCH: New York, 1994.
(36) Turkevich, J.; Stevenson, P. C.; Hillier, J. *Discuss. Faraday Soc.* **1951**, 55−75.
(37) Israelachvili, J. N. *Intermolecular Surface Forces*; Academic Press: San Diego, 1992.
(38) Murray, C. B.; Kagan, C. R.; Bawendi, M. G. *Annu. Rev. Mater. Sci.* **2000**, *30*, 545−610.
(39) Brust, M.; Walker, M.; Bethell, D.; Schiffrin, D. J.; Whyman, R. *J. Chem. Soc., Chem. Commun.* **1994**, 801−802.
(40) Marcus, M. A.; Flood, W.; Steigerwald, M.; Brus, L.; Bawendi, M. *J. Phys. Chem. B* **1991**, *95*, 1572−1576.
(41) Rogach, A. L.; Kornowski, A.; Gao, M. Y.; Eychmuller, A.; Weller, H. *J. Phys. Chem. B* **1999**, *103*, 3065−3069.
(42) Lawless, D.; Kapoor, S.; Meisel, D. *J. Phys. Chem. B* **1995**, *99*, 10329−10335.
(43) Lover, T.; Bowmaker, G. A.; Seakins, J. M.; Cooney, R. P. *Chem. Mater.* **1997**, *9*, 967−975.
(44) Mahamuni, S.; Khosravi, A. A.; Kundu, M.; Kshirsagar, A.; Bedekar, A.; Avasare, D. B.; Singh, P.; Kulkarni, S. K. *J. Appl. Phys.* **1993**, *73*, 5237−5240.
(45) Vogel, W.; Borse, P. H.; Deshmukh, N.; Kulkarni, S. K. *Langmuir* **2000**, *16*, 2032−2037.
(46) Fauconnier, N.; Pons, J. N.; Roger, J.; Bee, A. *J. Colloid Interface Sci.* **1997**, *194*, 427−433.
(47) Chen, S. W.; Huang, K.; Stearns, J. A. *Chem. Mater.* **2000**, *12*, 540−547.
(48) Collier, C. P.; Saykally, R. J.; Shiang, J. J.; Henrichs, S. E.; Heath, J. R. *Science* **1997**, *277*, 1978−1981.
(49) Hostetler, M. J.; Zhong, C. J.; Yen, B. K. H.; Anderegg, J.; Gross, S. M.; Evans, N. D.; Porter, M.; Murray, R. W. *J. Am. Chem. Soc.* **1998**, *120*, 9396−9397.
(50) Mayya, K. S.; Patil, V.; Sastry, M. *Langmuir* **1997**, *13*, 3944−3947.
(51) Yonezawa, T.; Sutoh, M.; Kunitake, T. *Chem. Lett.* **1997**, 619−620.
(52) Steigerwald, M. L.; Alivisatos, A. P.; Gibson, J. M.; Harris, T. D.; Kortan, R.; Muller, A. J.; Thayer, A. M.; Duncan, T. M.; Douglass, D. C.; Brus, L. E. *J. Am. Chem. Soc.* **1988**, *110*, 3046−3050.
(53) Templeton, A. C.; Wuelfing, M. P.; Murray, R. W. *Acc. Chem. Res.* **2000**, *33*, 27−36.
(54) Kim, B. S.; Avila, L.; Brus, L. E.; Herman, I. P. *Appl. Phys. Lett.* **2000**, *76*, 3715−3717.
(55) Glish, G. L.; Porter, M. D.; Evans, N. D.; Murray, R. W. *Langmuir* **1998**, *14*, 17−30.
(56) Hostetler, M. J.; Templeton, A. C.; Murray, R. W. *Langmuir* **1999**, *15*, 3782−3789.
(57) Chen, S. W.; Murray, R. W. *Langmuir* **1999**, *15*, 682−689.
(58) Hostetler, M. J.; Wingate, J. E.; Zhong, C. J.; Harris, J. E.; Vachet, R. W.; Clark, M. R.; Londono, J. D.; Green, S. J.; Stokes, J. J.; Wignall, G. D.; Glish, G. L.; Porter, M. D.; Evans, N. D.; Murray, R. W. *Langmuir* **1998**, *14*, 17−30.
(59) Templeton, A. C.; Chen, S. W.; Gross, S. M.; Murray, R. W. *Langmuir* **1999**, *15*, 66−76.
(60) Shon, Y. S.; Gross, S. M.; Dawson, B.; Porter, M.; Murray, R. W. *Langmuir* **2000**, *16*, 6555−6561.
(61) Cliffel, D. E.; Zamborini, F. P.; Gross, S. M.; Murray, R. W. *Langmuir* **2000**, *16*, 9699−9702.
(62) Zamborini, F. P.; Gross, S. M.; Murray, R. W. *Langmuir* **2001**, *17*, 481−488.
(63) Lover, T.; Henderson, W.; Bowmaker, G. A.; Seakins, J. M.; Cooney, R. P. *Chem. Mater.* **1997**, *9*, 1878−1886.
(64) Templeton, A. C.; Hostetler, M. J.; Warmoth, E. K.; Chen, S. W.; Hartshorn, C. M.; Krishnamurthy, V. M.; Forbes, M. D. E.; Murray, R. W. *J. Am. Chem. Soc.* **1998**, *120*, 4845−4849.
(65) Demers, L. M.; Mirkin, C. A.; Mucic, R. C.; Reynolds, R. A., III.; Letsinger, R. L.; Elghanian, R.; Viswanadham, G. *Anal. Chem.* **2000**, *72*, 5535−5541.
(66) Wuelfing, W. P.; Zamborini, F. P.; Templeton A. C.; Wen, X.; Yoon, H.; Murray, R. W. *Chem. Mater.* **2001**, *13*, 87−95.
(67) Brinker, C. J.; Lu, Y. F.; Sellinger, A.; Fan, H. Y. *Adv. Mater.* **1999**, *11*, 579−585.
(68) Potter, D. I. *J. Phys. Chem. B* **1999**, *103*, 7416−7428.

(69) Andres, R. P.; Bielefeld, J. D.; Henderson, J. I.; Janes, D. B.; Kolagunta, V. R.; Kubiak, C. P.; Mahoney, W. J.; Osifchin, R. G. *Science* **1996**, *273*, 1690−1693.
(70) Brooks, K.; Gratzel, M. *Chem. Mater.* **1998**, *10*, 2419−2425.
(71) Rajh, T.; Thurnauer, M. C.; Thiyagarajan, P.; Tiede, D. M. *J. Phys. Chem. B* **1999**, *103*, 2172−2177.
(72) Bright, R. M.; Musick, M. D.; Natan, M. J. *Langmuir* **1998**, *14*, 5695−5701.
(73) Yin, J. S.; Wang, Z. L. *Nanostructured Mater.* **1999**, *11*, 845−852.
(74) Park, S. H.; Xia, Y. N. *Langmuir* **1999**, *15*, 266−273.
(75) Chen, Y. Y.; Baker, G. L.; Ding, Y. Q.; Rabolt, J. F. *J. Am. Chem. Soc.* **1999**, *121*, 6962−6963.
(76) Kiely, C. J.; Fink, J.; Brust, M.; Bethell, D.; Schiffrin, D. J. *Nature* **1998**, *396*, 444−446.
(77) Whetten, R. L.; Khoury, J. T.; Alvarez, M. M.; Murthy, S.; Vezmar, I.; Wang, Z. L.; Stephens, P. W.; Cleveland, C. L.; Luedtke, W. D.; Landman, U. *Adv. Mater.* **1996**, *8*, 428+.
(78) Harfenist, S. A.; Wang, Z. L.; Alvarez, M. M.; Vezmar, I.; Whetten, R. L. *J. Phys. Chem. B* **1996**, *100*, 13904−13910.
(79) Schaaff, T. G.; Shafigullin, M. N.; Khoury, J. T.; Vezmar, I.; Whetten, R. L.; Cullen, W. G.; First, P. N.; Gutierrezwing, C.; Ascensio, J.; Joseyacaman, M. J. *J. Phys. Chem.* **1997**, *101*, 7885−7891.
(80) Alvarez, M. M.; Khoury, J. T.; Schaaff, T. G.; Shafigullin, M. N.; Vezmar, I.; Whetten, R. L. *J. Phys. Chem.* **1997**, *101*, 3706−3712.
(81) Whetten, R. L.; Shafigullin, M. N.; Khoury, J. T.; Schaaff, T. G.; Vezmar, I.; Alvarez, M. M.; Wilkinson, A. *Acc. Chem. Res.* **1999**, *32*, 397−406.
(82) Schaaff, T. G.; Whetten, R. L. *J. Phys. Chem. B* **2000**, *104*, 2630−2641.
(83) Bigioni, T. P.; Whetten, R. L.; Dag, O. *J. Phys. Chem. B* **2000**, *104*, 6983−6986.
(84) Breen, T. L.; Tien, J.; Oliver, S. R. J.; Hadzic, T.; Whitesides, G. M. *Science* **1999**, *284*, 948−951.
(85) Wei, Q. H.; Cupid, D. M.; Wu, X. L. *Appl. Phys. Lett.* **2000**, *77*, 1641−1643.
(86) Boal, A. K.; Ilhan, F.; DeRouchey, J. E.; Thurn-Albrecht, T.; Russell, T. P.; Rotello, V. M. *Nature* **2000**, *404*, 746−748.
(87) Adachi, E. *Langmuir* **2000**, *16*, 6460−6463.
(88) Meldrum, F. C.; Fendler, J. H. *Construction of Organized Particulate Films by the Langmuir−Blodgett Technique*; VCH: New York, 1996; pp 175−219.
(89) Sato, T.; Brown, D.; Johnson, B. F. G. *Chem. Commun.* **1997**, 1007−1008.
(90) Brust, M.; Bethell, D.; Kiely, C. J.; Schiffrin, D. J. *Langmuir* **1998**, *14*, 5425−5429.
(91) Brust, M.; Bethell, D.; Schiffrin, D. J.; Kiely, C. *J. Adv. Mater.* **1995**, *7*, 795+.
(92) Fan, H. Y.; Lopez, G. P. *Langmuir* **1997**, *13*, 119−121.
(93) Baum, T.; Bethell, D.; Brust, M.; Schiffrin, D. J. *Langmuir* **1999**, *15*, 866−871.
(94) Gomez, S.; Philippot, K.; Colliere, V.; Chaudret, B.; Senocq, F.; Lecante, P. *Chem. Commun.* **2000**, 1945−1946.
(95) Maoz, R.; Matlis, S.; DiMasi, E.; Ocko, B. M.; Sagiv, J. *Nature* **1996**, *384*, 150−153.
(96) Maoz, R.; Sagiv, J. *Adv. Mater.* **1998**, *10*, 580−584.
(97) Mirkin, C. A.; Letsinger, R. L.; Mucic, R. C.; Storhoff, J. J. *Nature* **1996**, *382*, 607−609.
(98) Herne, T. M.; Tarlow, M. J. *J. Am. Chem. Soc.* **1997**, *119*, 8916−8920.
(99) Mucic, R. C.; Storhoff, J. J.; Mirkin, C. a.; Letsinger, R. L. *J. Am. Chem. Soc.* **1998**, *120*, 12674−12675.
(100) Boncheva, M.; Scheibler, L.; Lincoln, P.; Vogel, H.; Akerman, B. *Langmuir* **1999**, *15*, 4317−4320.
(101) Storhoff, J. J.; Mirkin, C. A. *Chem. Rev.* **1999**, *99*, 1849−1862.
(102) O'Brien, J. C.; Stickney, J. T.; Porter, M. D. *Langmuir* **2000**, *16*, 9559−9567.
(103) Beermann, N.; Vayssieres, L.; Lindquist, S. E.; Hagfeldt, A. *J. Electrochem. Soc.* **2000**, *147*, 2456−2461.
(104) Okahata, Y.; Matsunobu, Y.; Ijiro, K.; Mukae, M.; Murakami, A.; Makino, K. *J. Am. Chem. Soc.* **1992**, *114*, 8299−8300.
(105) Peterlinz, K. A.; Georgiadis, R. M.; Herne, T. M.; Tarlov, M. J. *J. Am. Chem. Soc.* **1997**, *119*, 3401−3402.
(106) Caruso, F.; Rodda, E.; Furlong, D. N.; Niikura, K.; Okahata, Y. *Anal. Chem.* **1997**, *69*, 2043−2049.
(107) Lin, X. M.; Parthasarathy, R.; Jaeger, H. M. *Appl. Phys. Lett.* **2001**, *78*, 1915−1917.
(108) Borgstrom, M.; Johansson, J.; Samuelson, L.; Seifert, W. *Appl. Phys. Lett.* **2001**, *78*, 1367−1369.
(109) Iler, R. K. *J. Colloid Interface Sci.* **1966**, *21*, 569−594.
(110) Lee, H.; Kepley, L. J.; Hong, H.-G.; Mallouk, T. E. *J. Am. Chem. Soc.* **1988**, *110*, 618−620.
(111) Decher, G.; Hong, J. D. *Ber. Bunsen-Ges. Phys. Chem.* **1991**, *11*, 1430−1434.
(112) Lvov, Y.; Haas, H.; Decher, G.; Mohwald, H.; Kalachev, A. *J. Phys. Chem. B* **1993**, *97*, 12835−12841.
(113) Fendler, J. H. *Chem. Mater.* **1996**, *8*, 1616−1624.
(114) Brumfield, J. C.; Goss, C. A.; Irene, A. E.; Murray, R. W. *Langmuir* **1992**, *8*, 2810−2817.
(115) Bard, A. J.; Mallouk, T. *Electrodes modified with clays, zeolites, and related microporous solids*; Murray, R. W., Ed.; John Wiley & Sons: New York, 1992; Vol. XXII, pp 270−312.
(116) Mallouk, T. E.; Kim, H.-N.; Ollivier, P. J.; Keller, S. W. *Ultrathin Films based on Layered Inorganic Solids*; Mallouk, T. E., Kim, H.-N., Ollivier, P. J., Keller, S. W., Eds.; Pergamon Press: Oxford, 1996; Vol. 7, p 189.
(117) Decher, G. *Layered Nanoarchitectures via Directed Assembly of Anionic and Cationic Molecules*; Sauvage, J.-P., Ed.; Pergamon Press: Oxford, 1996; Vol. 9, pp 507−528.
(118) Correa-Duarte, M. A.; Giersig, M.; Kotov, N. A.; Liz-Marzan, L. M. *Langmuir* **1998**, *14*, 6430−6435.
(119) http://www.chem.fsu.edu/multilayers/.
(120) Keller, S. W.; Kim, H. N.; Mallouk, T. E. *J. Am. Chem. Soc.* **1994**, *116*, 8817−8818.
(121) Campbell, I. H.; Kress, J. D.; Martin, R. L.; Smith, D. L.; Barashkov, N. N.; Ferraris, J. P. *Appl. Phys. Lett.* **1997**, *71*, 3528−3530.
(122) Ratner, M. A.; Jortner, J. *Molecular Electronics*; Blackwell Science, Ltd.: London, UK, 1997.
(123) Noh, M.; Johnson, C. D.; Hornbostel, M. D.; Thiel, J.; Johnson, D. C. *Chem. Mater.* **1996**, *8*, 1625−1635.
(124) Zhou, C.; Deshpande, M. R.; Reed, M. A.; Jones, L.; Tour, J. M. *Appl. Phys. Lett.* **1997**, *71*, 611−613.
(125) Collett, J.; Vuillaume, D. *Appl. Phys. Lett.* **1998**, *73*, 2681−2683.
(126) Cygan, M. T.; Dunbar, T. D.; Arnold, J. J.; Bumm, L. A.; Shedlock, N. F.; Burgin, T. P.; Jones, L., II; Allara, D. L.; Tour, J. M.; Weiss, P. S. *J. Am. Chem. Soc.* **1998**, *120*, 2721−2732.
(127) Grobert, N.; Mayne, M.; Terrones, M.; Sloan, J.; Dunin-borkowski, R. E.; Kamalakaran, R.; Seeger, T.; Terrones, H.; Ruhle, M.; Walton, D. R. M.; Kroto, H. W.; Hutchison, J. L. *Chem. Commun.* **2001**, 471−472.
(128) Zhang, Y.; Dai, H. *J. Appl. Phys. Lett.* **2000**, *77*, 3015−3017.
(129) Braun, E.; Eichen, Y.; Sivan, U.; Ben-Yoseph, G. *Nature* **1998**, *391*, 775−778.
(130) Feldheim, D. L.; Keating, C. D. *Chem. Soc. Rev.* **1998**, *27*, 1−12.
(131) Wold, D. J.; Frisbie, C. D. *J. Am. Chem. Soc.* **2000**, *122*, 2970−2971.
(132) Fan, F. R. F.; Yang, J. P.; Dirk, S. M.; Price, D. W.; Kosynkin, D.; Tour, J. M.; Bard, A. J. *J. Am. Chem. Soc.* **2001**, *123*, 2454−2455.
(133) Haag, R.; Rampi, M. A.; Holmlin, R. E.; Whitesides, G. M. *J. Am. Chem. Soc.* **1999**, *121*, 7895−7906.
(134) Finklea, H. O.; Liu, L.; Ravenscroft, M. S.; Punturi, S. *J. Phys. Chem. B* **1996**, *100*, 18852−18858.
(135) Weber, K. S.; Creager, S. E. *J. Electroanal. Chem.* **1998**, *458*, 17−22.
(136) Kondo, T.; Yanagida, M.; Nomura, S.; Ito, T.; Uosaki, K. *J. Electroanal. Chem.* **1997**, *438*, 121−126.
(137) Walter, D. G.; Campbell, D. J.; Mirkin, C. A. *J. Phys. Chem. B* **1999**, *103*, 402−405.
(138) Skulason, H.; Frisbie, C. D. *Langmuir* **1998**, *14*, 5834−5840.
(139) Lindgren, A.; Larsson, T.; Ruzgas, T.; Gorton, L. *J. Electroanal. Chem.* **2000**, *494*, 105−113.
(140) Imahori, H.; Norieda, H.; Yamada, H.; Nishimura, Y.; Yamazaki, I.; Sakata, Y.; Fukuzumi, S. *J. Am. Chem. Soc.* **2001**, *123*, 100−110.
(141) Sagvolden, G.; Giaever, I.; Feder, J. *Langmuir* **1998**, *14*, 5984−5987.
(142) Ogawa, S.; Hu, K.; Fan, F. R. F.; Bard, A. J. *J. Phys. Chem. B* **1997**, *101*, 5707−5711.
(143) Liu, J.; Lee, T.; Janes, D. B.; Walsh, B. L.; Melloch, M. R.; Woodall, J. M.; Reifenberger, R.; Andres, R. P. *Appl. Phys. Lett.* **2000**, *77*, 373−375.
(144) Cassagneau, T.; Mallouk, T. E.; Fendler, J. H. *J. Am. Chem. Soc.* **1998**, *120*, 7848−7859.
(145) Sze, S. M. *Tunnel Devices*; J. Wiley: New York, 1981.
(146) Sweryda-Krawiec, B.; Cassagneau, T.; Fendler, J. H. *Adv. Mater.* **1999**, *11*, 659−664.
(147) Pardo-yissar, V.; Katz, E.; Lioubashevski, O.; Willner, I. *Langmuir* **2001**, *17*, 1110−1118.
(148) Blonder, R.; Levi, S.; Tao, G. L.; Ben-dov, I.; Willner, I. *J. Am. Chem. Soc.* **1997**, *119*, 10467−10478.
(149) Patolsky, F.; Katz, E.; Heleg-shabtai, V.; Willner, I. *Chem.−Eur. J.* **1998**, *4*, 1068−1073.
(150) Lahav, M.; Gabai, R.; Shipway, A. N.; Willner, I. *Chem. Commun.* **1999**, 1937−1938.
(151) Shipway, A. N.; Lahav, M.; Willner, I. *Adv. Mater.* **2000**, *12*, 993−998.
(152) Lahav, M.; Kharitonov, A. B.; Katz, O.; Kunitake, T.; Willner, I. *Anal. Chem.* **2001**, *73*, 720−723.
(153) Willner, I.; Willner, B. *Adv. Mater.* **1995**, *7*, 587−589.
(154) Willner, I.; Willner, B. *J. Mater. Chem.* **1998**, *8*, 2543−2556.
(155) Willner, I.; Pardo-yissar, V.; Katz, E.; Ranjit, K. T. *J. Electroanal. Chem.* **2001**, *497*, 172−177.
(156) Lahav, M.; Gabriel, T.; Shipway, A. N.; Willner, I. *J. Am. Chem. Soc.* **1999**, *121*, 258−259.

(157) Lahav, M.; Heleg-shabtai, V.; Wasserman, J.; Katz, E.; Willner, I.; Durr, H.; Hu, Y. Z.; Bossmann, S. H. *J. Am. Chem. Soc.* **2000**, *122*, 11480−11487.
(158) Andres, R. P.; Bein, T.; Dorogi, M.; Feng, S.; Henderson, J. I.; Kubiak, C. P.; Mahoney, W.; Osifchin, R. G.; Reifenberger, R. *Science* **1996**, *272*, 1323−1325.
(159) von Klitzing, K. *J. Appl. Phys.* **1999**, *85*, 3374−3376.
(160) Schaadt, D. M.; Yu, E. T.; Sankar, S.; Berkowitz, A. E. *Appl. Phys. Lett.* **1999**, *74*, 472−474.
(161) Persson, S. H. M.; Olofsson, L.; Gunnarsson, L. *Appl. Phys. Lett.* **1999**, *74*, 2546−2548.
(162) Bezryadin, A.; Dekker: C.; Schmid, G. *Appl. Phys. Lett.* **1997**, *71*, 1273−1275.
(163) Markovich, G.; Leff, D. V.; Chung, S. W.; Soyez, H. M.; Dunn, B.; Heath, J. R. *Appl. Phys. Lett.* **1997**, *70*, 3107−3109.
(164) Facci, P.; Erokhin, V.; Carrara, S.; Nicolini, C. *Proc. Natl. Acad. Sci. U.S.A.* **1996**, *93*, 10556−10559.
(165) Brousseau, L. C., III.; Zhao, Q.; Shultz, D. A.; Feldheim, D. L. *J. Am. Chem. Soc.* **1998**, *120*, 7645−7646.
(166) Park, K. H.; Ha, J. S.; Yun, W. S.; Shin, M.; Park, K. W.; Lee, E. H. *Appl. Phys. Lett.* **1997**, *71*, 1469−1471.
(167) Sato, T.; Ahmed, H.; Brown, D.; Johnson, B. F. G. *J. Appl. Phys.* **1997**, *82*, 696−701.
(168) Han, M. Y.; Zhou, L.; Quek, C. H.; Li, S. F. Y.; Huang, W. *Chem. Phys. Lett.* **1998**, *287*, 47−52.
(169) Hutchison, K.; Gao, J.; Schick, G.; Rubin, Y.; Wudl, F. *J. Am. Chem. Soc.* **1999**, *121*, 5611−5612.
(170) Ingram, R. S.; Hostetler, M. J.; Murray, R. W.; Schaaf, T. G.; Khoury, J. T.; Whetten, R. L.; Bigioni, T. P.; Guthrie, D. K.; First, P. N. *J. Am. Chem. Soc.* **1997**, *119*, 9279−9280.
(171) Chen, S. W.; Murray, R. W.; Feldberg, S. W. *J. Phys. Chem. B* **1998**, *102*, 9898−9907.
(172) Chen, S. W.; Ingram, R. S.; Hostetler, M. J.; Pietron, J. J.; Murray, R. W.; Schaaff, T. G.; Khoury, J. T.; Alvarez, M. M.; Whetten, R. L. *Science* **1998**, *280*, 2098−2101.
(173) Zamborini, F. P.; Hicks, J. F.; Murray, R. W. *J. Am. Chem. Soc.* **2000**, *122*, 4514−4515.
(174) Jang, J. S.; Lim, B.; Lee, J.; Hyeon, T. *Chem. Commun.* **2001**, *12*, 83−84.
(175) Ashoori, R. C. *Nature* **1996**, *379*, 413−419.
(176) Schedelbeck, G.; Wegscheider, W.; Bichler, M.; Abstreiter, G. *Science* **1997**, *278*, 1792−1795.
(177) Hijman, R. V.; Tarucha, S.; Kouwenhoven, L. P. *Nature* **1998**, *395*, 873−876.
(178) Banin, U.; Cao, Y. W.; Katz, D.; Millo, O. *Nature* **1999**, *400*, 542−544.
(179) Shim, M.; Guyot-sionnest, P. *Nature* **2000**, *407*, 981−983.
(180) Bayer, M.; Stern, O.; Hawrylak, P.; Fafard, S.; Forchel, A. *Nature* **2000**, *405*, 923−926.
(181) Zrenner, A. *J. Chem. Phys.* **2000**, *112*, 7790−7798.
(182) Feldheim, D. L.; Grabar, K. C.; Natan, M. J.; Mallouk, T. E. *J. Am. Chem. Soc.* **1996**, *118*, 7640−7641.
(183) Tour, J. M.; Kozaki, M.; Seminario, J. M. *J. Am. Chem. Soc.* **1998**, *120*, 8486−8493.
(184) Metzger, R. M. *Acc. Chem. Res.* **1999**, *32*, 950−957.
(185) Chen, J.; Reed, M. A.; Rawlett, A. M.; Tour, J. M. *Science* **1999**, *286*, 1550−1552.
(186) Tour, J. M. *Acc. Chem. Res.* **2000**, *33*, 791−804.
(187) Jortner, J.; Ratner, M. *Molecular Electronics*; Blackwell, London, 1997.

CM010165M